Journal of Photochemistry and Photobiology A: Chemistry 298 (2014) 24–32

Contents lists available at ScienceDirect

Journal of Photochemistry and Photobiology A: Chemistry

journal homepage: www.elsevier.com/locate/jphotochem

Photocatalytic oxidation of pirimicarb in aqueous slurries containing binary and ternary oxides of zinc and titanium

José Fenoll [a,*], Isabel Garrido [a], Pilar Hellín [a], Pilar Flores [a], Nuria Vela [b], Simón Navarro [c]

[a] Departamento de Calidad y Garantía Alimentaria, Instituto Murciano de Investigación y Desarrollo Agrario y Alimentario (IMIDA), C/Mayor s/n. La Alberca, 30150 Murcia, Spain
[b] Facultad de Enfermería, Universidad Católica San Antonio de Murcia, Campus de Los Jerónimos, s/n. Guadalupe, 30107, Murcia, Spain
[c] Departamento de Química Agrícola, Geología y Edafología, Facultad de Química, Universidad de Murcia, Campus Universitario de Espinardo, 30100, Murcia, Spain

ARTICLE INFO

Article history:
Received 27 June 2014
Received in revised form 10 October 2014
Accepted 17 October 2014
Available online 22 October 2014

Keywords:
Pirimicarb
Transformation products
Photocatalytic Oxidation
Semiconductor materials

ABSTRACT

The photocatalytic degradation of pirimicarb in pure water has been studied using zinc oxide (ZnO), titanium dioxide (TiO_2) and zinc titanates (Zn_2TiO_4 and $ZnTiO_3$) under artificial light (300–460 nm) irradiation. Comparison of catalysts showed that TiO_2 is the most efficient for the removal of pirimicarb and their transformation products. To obtain a better understanding of the mechanistic details of these ZnO–TiO_2-assisted photodegradation of pirimicarb, the transformation products of the processes were identified by liquid chromatography tandem mass spectrometry (LC-MS^2) and liquid chromatography time of flight mass spectrometry (LC-TOF/MS) techniques. The probable photodegradation pathways are proposed and discussed. The main steps involved: N-dealkylation of the 2-dimethylamino group to form the carbamate and decarbamoylation of the carbamate moiety with further N-dealkylation of the 2-dimethylamino group to have the hydroxypyrimidines.

1. Introduction

Carbamate pesticides have been extensively used in pest control owing to their high effectiveness and low persistence. Pirimicarb (2-dimethylamino-5,6-dimethylpyrimidin-4-yldimethylcarbamate) is an *N*,*N*-dimethylcarbamate insecticide that is widely employed against aphids in fruit and vegetable. Pirimicarb exerts its toxic effects by inhibiting the enzyme acetylcholinesterase [1]. This systemic insecticide is suspected carcinogen and mutagen [2]. In addition, their high solubility, pirimicarb may leach through the soil profile [3,4]. Consequently, it is of primary importance to apply remediation strategies to polluted waters in order to protect hydric resources.

In this context, the degradation of organic pollutants in water by photocatalysis, using semiconductors such as TiO_2 and ZnO, has been widely used by numerous authors in the past two decades [5–9]. Solar radiation, a renewable source of energy, inexhaustible and pollution-free, can be widely utilized in the photocatalytic degradation of the dyes, pesticides and detergents [10–13]. The photocatalytic process is based on the generation of electron–hole pairs by irradiation of semiconductor particles with energy $h\nu \geq E_g$ (band gap energy). These electron–hole pairs are capable of initiating a series of chemical reactions that eventually mineralize the pollutants [14].

These semiconductors have many advantages such as a low price, high photocatalytic activity, simple preparation, etc. However, ZnO has a low stability at high pH, while TiO_2 can only absorb a small portion of solar spectra in the UV region [15]. Thus, the photocatalytic activity of ZnO–TiO_2 systems (Zn_2TiO_4 with cubic spinel crystal structure, $Zn_2Ti_3O_8$ with cubic defect spinel structure and $ZnTiO_3$ with cubic or hexagonal structure) is being investigated with the purpose of looking for more efficient materials for photocatalytic applications [16–18]. Although the photocatalytic degradation of pirimicarb using ZnO and TiO_2 has been studied from previous researchers [5,19], the effect of ZnO–TiO_2 system for the removal of pirimicarb from water has not been studied. The main goal of this work was to assess the effectiveness of the photocatalytic process for the decontamination of water polluted by pirimicarb, to evaluate the kinetics aspects of the process and the reaction intermediates for understanding the mechanistic details of the photodegradation in the ZnO–TiO_2 systems (ZnO, TiO_2, Zn_2TiO_4 and $ZnTiO_3$).

---

* Corresponding author: Tel.: +34 968366798; fax: +34 968366792.
E-mail address: jose.fenoll@carm.es (J. Fenoll).

http://dx.doi.org/10.1016/j.jphotochem.2014.10.014

2. Experimental

2.1. Pirimicarb, transformation products and reagents

Analytical reagents were purchased from Dr. Ehrenstorfer (Augsburg, Germany) with purity >99%. Pirimicarb and their main organic transformation products are listed in Table 1. Zinc oxide (ZnO) and zinc titanium oxide (Zn_2TiO_4) were purchased from Alfa Aesar (Karlsruhe, Germany). zinc titanate ($ZnTiO_3$) was purchased from Sigma–Aldrich Química S.A. (Madrid, Spain). Titanium dioxide P25 Degussa (TiO_2) was supplied from Nippon Aerosil Co., Ltd. (Osaka, Japan). Acetonitrile was supplied by Scharlau (Barcelone, Spain).

2.2. Photocatalyst characterization

The photocatalysts were characterized by a PerkinElmer Lambda 750S UV/VIS spectrophotometer equipped with 60 mm integrating sphere accessory for diffuse reflectance spectra. Software: UV WinLab DPV 1.0 (Shelton, USA). A $BaSO_4$ standard was used as the reference spectrum. The crystalline structure of the phatacatalysts was characterized by means of powder X-ray diffractometry (XRD), on a Philips PW 1700. The samples were measured at 40 kV and 24 mA using Cu-Kα radiation at a scanning speed of 1° (2θ). The morphology of the solids was examined by field emission scanning electron microscopy (FE-SEM) using a Carl Zeiss MERLIN VP Compact microscope (Oberkochem, Germany) with high resolution imaging up to 0.8 nm @15 KV, acceleration voltage of 0.02–30 kV and energy dispersive X-ray (EDX) attached to SEM. The surface area (S_{BET}) of the semiconductors was measured according to the BET method by nitrogen adsorption–desorption isotherms at 77 K on a Micromeritics Tristar 3000 instrument (Micromeritics Instruments Co., USA).

2.3. Photoreactor setup

The photocatalytic and photolytic experiments were performed in a photochemical reactor [20]. The reactant solution containing different amounts of the semiconductor powder (100–400 mg L^{-1}) was circulated at a flow rate of 600 mL min^{-1}.

Initially, 2000 mL of type II analytical-grade water (pH 7.1, ORP 212 mV, resistivity >5 MΩ cm (25 °C); conductivity <1 μS cm^{-1}, TOC <30 μg L^{-1}; microorganisms < 10 cfu mL^{-1}) was mixed with commercial product (APHOX, Syngenta) to reach a spiking level of about 0.1 mg L^{-1} of pirimicarb, homogenizing the mixture for 20 min to constant concentration in the dark. After this time the appropriate amount of catalyst (200 mg L^{-1}) was added to the reaction solution. The respective mixtures were maintained for 30 min in the dark, prior to illumination, in order to achieve the maximum adsorption of pirimicarb onto semiconductor surface. Several samples from 0 to 60 min were taken during the illumination period. In all cases, assays were replicated three times.

2.4. Analytical determinations

The extraction procedure involves a pre-concentration of pirimicarb from water samples (50 mL) step based on solid-phase extraction with a silica-based bonded C_{18} cartridge (Sep-Pak Plus 500 mg, 6 mL, Waters). The SPE cartridge was first conditioned with 5 mL of acetonitrile, followed by 5 mL of deionised water. Extraction of water samples was carried out at a 8 mL min^{-1} flow rate. The samples were loaded onto the cartridges, and washed with deionised water and dried for 15 min under a vacuum. The analytes retained were eluted with 5 mL of acetonitrile. The solution was filtered through a 0.45 μm filter and analyzed by LC-MS^2 according to the procedure described by Fenoll et al. [21]

Analysis of pirimicarb and their transformed products: 2-[(methylformyl) amino]-5,6-dimethylpyrimidin-4-yl dimethylcarbamate (Metabolite I), 2-(dimethylamino)-5,6-dimethyl-4-hydroxypyrimidine (Metabolite II), 2-(methylamino)-5,6-dimethyl-4-hydroxipirimidine (Metabolite III) and 2-(methylamino)-5,6 dimethylpyrimidin-4-yl dimethylcarbamate (MetaboliteV) was achieved by comparison with commercially available standards using an HPLC system (Agilent Series 1100, Agilent Technologies, Santa Clara, CA, USA) equipped with a G6410A triple quadrupole mass spectrometer. A preliminary study of the optimal single reaction monitoring (SRM) transitions for each compound was carried out by injecting individual analytes at a concentration level of 10 μg mL^{-1}. Various fragmentor voltages (FV) and collision energies (CE) were applied to

Table 1
Analytical conditions of pirimicarb and their transformation products by HPLC-MS^2 and HPLC-TOF/MS.

Compounds	MF[a]	t_r[b](min)	HPLC-MS^2						HPLC-TOF/MS			
									m/z		Error (ppm)	DBE
			SRM$_1$[c]	F$_1$[d](V)	CE$_1$[e](V)	SRM$_2$[c]	F$_2$[d](V)	CE$_2$[e](V)	Theorical	Experimental		
Pirimicarb(2-(dimethylamino)-5,6-dimethylpyrimidin-4-yl dimethylcarbamate)	$C_{11}H_{18}N_4O_2$	13.7	239 → 72	90	20	239 → 182	90	15	239.1503	239.1504	−0.77	5
Metabolite I(2-[(methylformyl) amino]-5,6-dimethylpyrimidin-4-yl dimethylcarbamate)	$C_{11}H_{16}N_4O_3$	18.9	253 → 72	110	10	253 → 225	110	5	253.1295	253.1294	0.31	6
Metabolite II(2-(dimethylamino)-5,6-dimethyl-4-hydroxypyrimidine)	$C_8H_{13}N_3O$	3.25	168 → 98	110	20	168 → 71	110	30	168.1131	168.1132	−0.41	4
Metabolite III(2-(methylamino)-5,6-dimethyl-4-hydroxypirimidine)	$C_7H_{11}N_3O$	3.1	154 → 98	110	20	154 → 137	110	10	154.0975	154.0967	4.81	4
Metabolite IV(2-(formylamino)-5,6-dimethylpyrimidin-4-yl dimethylcarbamate)	$C_{10}H_{14}N_4O_3$	16.0	239 → 166	90	10	239 → 72	90	20	239.1139	239.1136	0.93	6
Metabolite V(2-(methylamino)-5,6 dimethylpyrimidin-4-yl dimethylcarbamate)	$C_{10}H_{16}N_4O_2$	11.2	225 → 168	110	10	225 → 72	110	20	225.1346	225.1348	−1.06	5

[a] Molecular formula.
[b] Retention time.
[c] Transitions (*m/z*).
[d] Fragmentor.
[e] Collision energy.

the compounds under study. Table 1 lists the pesticides along with their retention times and optimized SRM transitions with a dwell time of 60 ms.

Blank samples were used to establish the limit of detection (LOD) and the limit of quantification (LOQ). Both, LODs and LOQs were calculated from the signal-to-noise (S/N) ratio 3 and 10, respectively. The calibration samples were analyzed by spiking pesticides at 0.5–200 $\mu g L^{-1}$ levels into water samples in five replicates. The correlation coefficient was found to be >0.99 and the limits of quantification were in the range 5–50 $ng L^{-1}$ for

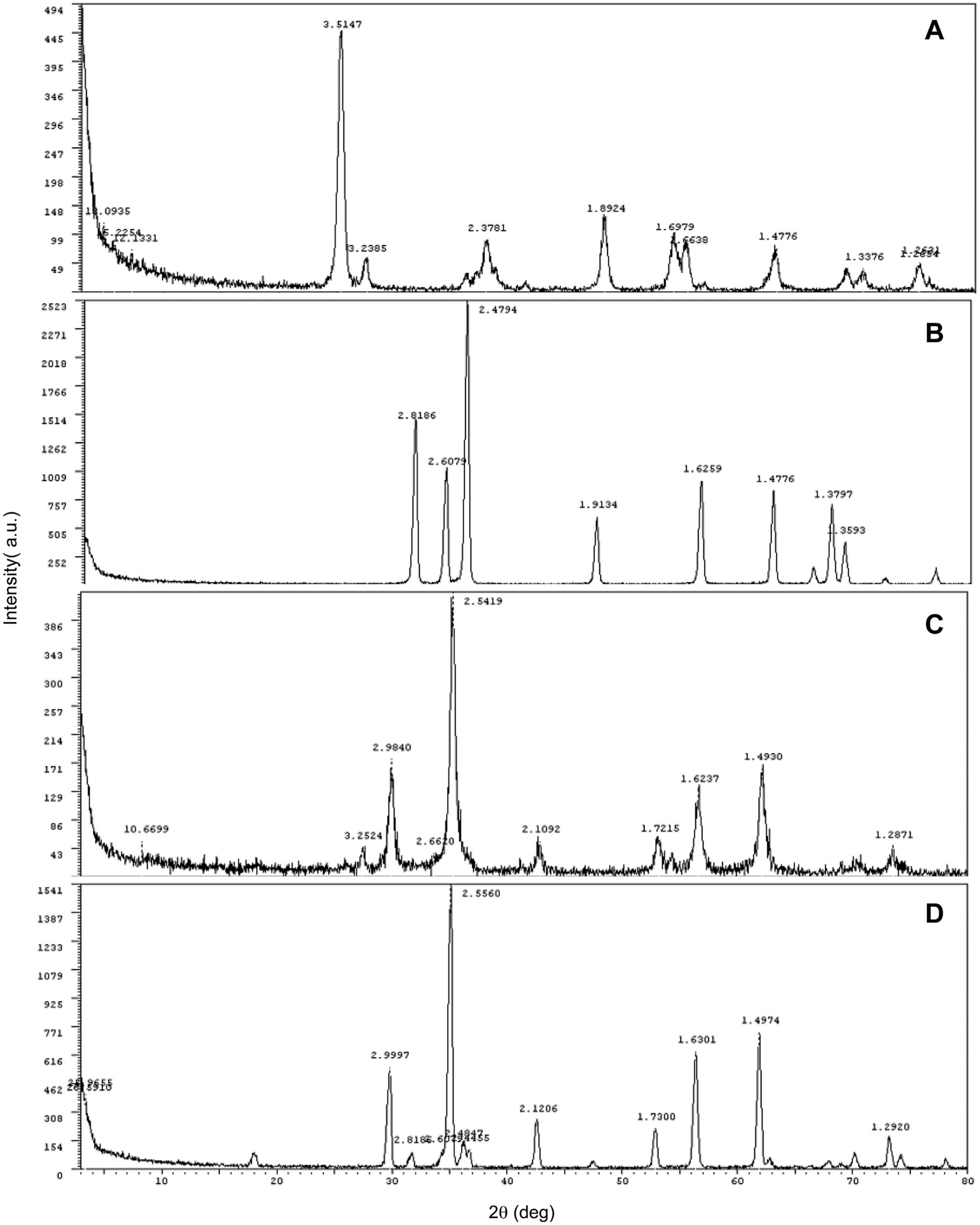

Fig. 1. XRD patterns of TiO_2 P25 Degussa (A), ZnO (B), $ZnTiO_3$(C) and Zn_2TiO_4(D).

Table 2
Physico-chemical properties and band gaps of studied photocatalysts.

	Photocatalysts			
	TiO_2 P25 Degussa	ZnO	Zn_2TiO_4	$ZnTiO_3$
Composition compounds				
TiO_2(%)	100		37.32	51.68
ZnO(%)		100	62.68	48.32
Particle size (nm)	32 ± 5	194 ± 16	4125 ± 650	56 ± 7
BET surface ($m^2 g^{-1}$)	55 ± 6	7 ± 1	0.6 ± 0.2	45 ± 8
Band-gap energy (eV)	3.0	3.1	3.3	2.8

pirimicarb and 2-(methylamino)-5,6-dimethyl-4-hydroxypirimidine (Metabolite III), respectively.

For other products, identification was carried out using an HPLC system connected to a TOF/MS (Agilent Technologies). Liquid chromatography was performed under the same conditions used in LC-MS^2.

A Shimadzu TOC-L Analyzer (Kyoto, Japan) equipped with an NDIR detector (680 °C combustion catalytic oxidation technique) was used. The DOC (dissolved organic carbon) procedure requires the sample be passed through a 0.45-μm filter prior to analysis to remove particulate OC from the sample.

2.5. Statistical analysis

The curve fitting and statistical data were obtained using SigmaPlot version 12.0 statistical software (Systat, Software Inc., San Jose, CA).

3. Results and discussion

3.1. XRD, SEM, UV–VIS diffuse reflectance spectra, percentages of TiO_2 and ZnO, BET surface area, and band gap

The degree of crystallinity, the particle size and the surface area of the catalysts can significantly influence the efficiency of photocatalytic oxidation of water contaminants. The X-ray diffractograms of ZnO–TiO_2 systems are given in Fig. 1. The contents of anatase (A) and rutile (R) phases in TiO_2 P25 Degussa powder was 70A:30R. ZnO was hexagonal wurtzite structure, while Zn_2TiO_4 and $ZnTiO_3$ powders were cubic structure. Table 2 presents the percentages of TiO_2 and ZnO, particle size and BET surface area of the studied photocatalysts. In comparison, SEM showed that the ZnO nanoparticles were predominantly smaller than 200 nm in diameter with hexagonal structure (Fig. 2B) whereas, some larger particles (Zn_2TiO_4) or agglomerates of TiO_2 and $ZnTiO_3$ nanoparticles were observed (Fig 2A, C and D)

The optical properties were studied by UV–vis diffuse reflectance (UV-DR) spectroscopy for TiO_2 P25 Degussa, ZnO, Zn_2TiO_4 and $ZnTiO_3$ samples. The diffuse reflectance spectra of different ZnO–TiO_2 systems are illustrated in Fig. 3. The direct band gaps energy was calculated by plotting $[F(R)\ h\nu]^{1/2}$ vs. $[h\nu - E_g]$, where $F(R) = (1 - R)^2/(2R)$, h is Plank's constant, E_g is the band gap energy, ν is the frequency of light and R is diffuse reflectance based on the Kubelka–Monk theory of diffuse reflectance. The indirect band gap estimated from the intercept of the tangents to the plots were 3.0, 3.1, 3.3 and 2.8 eV for the samples of TiO_2 P25 Degussa, ZnO, Zn_2TiO_4 and $ZnTiO_3$, respectively, which are consistent with the experimental band gaps determined by other authors [22–26].

3.2. Effect of catalyst concentration and initial pH during the photocatalytic degradation of pirimicarb

The catalyst concentration and the initial pH of the solution are two important parameters in the evaluation of photocatalytic reactions [26]. The effect of these two parameters on the photocatalytic degradation of pirimicarb has been investigated using a multivariate method. Minimum differences were observed in pH values during the irradiation time. Fig. 4 shows the response surface diagram obtained. In general, the rate constant initially increases by increasing the catalyst concentration. However, above a certain catalyst concentration a negative effect is observed. This unfavourable effect could be due to light scattering and the reduction of light penetration at a relatively high catalyst loading [27,28]. The optimum value for catalyst concentration was

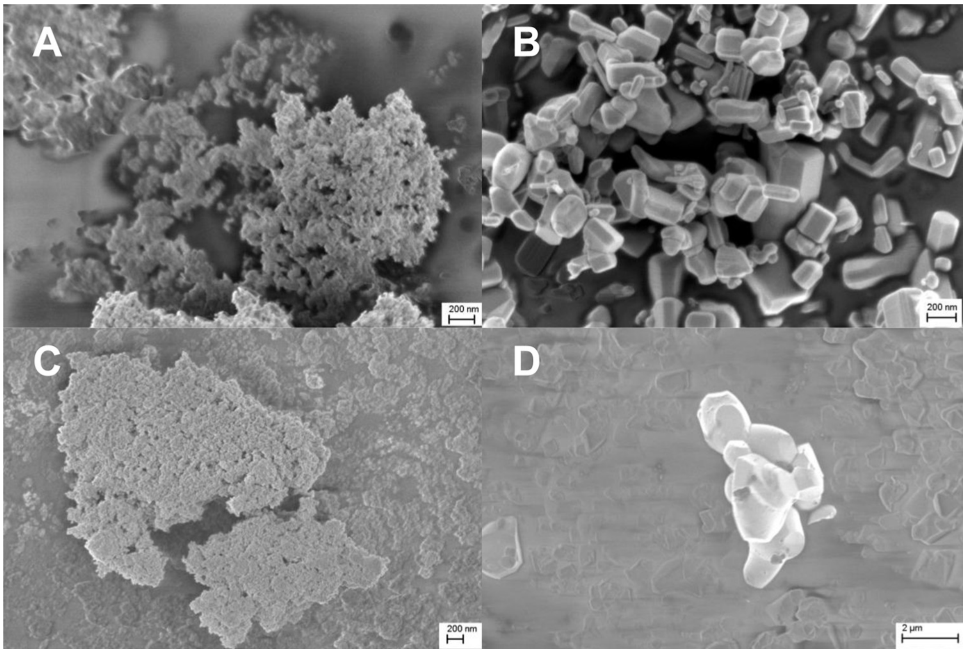

Fig. 2. SEM images of TiO_2 P25 Degussa (A), ZnO (B), $ZnTiO_3$(C) and Zn_2TiO_4(D).

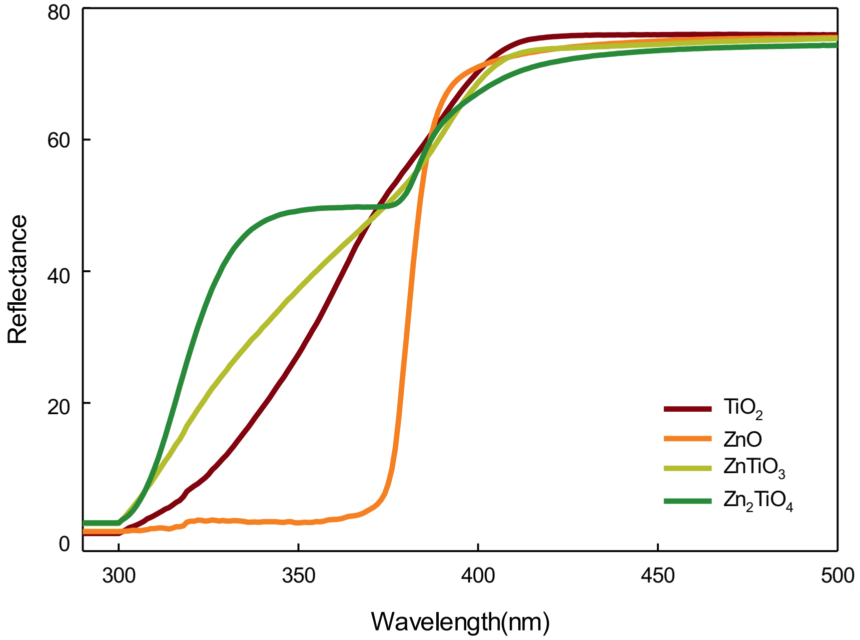

Fig. 3. Diffuse reflectance spectra of different catalysts (TiO_2 P25 Degussa, ZnO, $ZnTiO_3$ and Zn_2TiO_4).

200 mg L^{-1} for all the ZnO–TiO_2 systems. As consequence, further assays were carried out at this catalyst loading.

The influence of the initial pH value on the rate constant of the process using different ZnO–TiO_2 systems was also investigated. In general, at relatively low pH values, pirimicarb ($pK_a = 4.4$) might be protonated, which could provoke repulsion between the substrate and catalyst according to point of zero charge (PZC) of catalyst. As reported, the pH of the suspension in the case of TiO_2 P25 Degussa, Zn_2TiO_4 and $ZnTiO_3$ appeared to have an insignificant effect on the rate of disappearance of pirimicarb between pH 5.0 and pH 9.0. The PZC of TiO_2 depends on the production method the most frequent value for TiO_2 P25 and ZnO are 6.3 and 9.0, respectively [29], below or above which the catalyst surface is positively or negatively charged, respectively. Therefore, adsorption is an important parameter in the apparent kinetic order of degradation. Apparent half-order kinetics for TiO_2 suggests dissociative adsorption [30]. Moreover, the pH of the solution affects the formation of OH by the reaction between OH- and photo-induced holes on the TiO_2 surface. The h^+ are considered to be mainly responsible for oxidation at low pH, whereas OH are considered as the predominant species in neutral or alkaline medium [31]. In case of ZnO, the optimum value for initial pH was 7.0, it can be due to acid–base properties of this catalyst [32]. Bearing in mind the results obtained for ZnO and the insignificant effect on the rate of disappearance of pirimicarb between pH 5.0 and pH 9.0 for TiO_2 P25 Degussa, Zn_2TiO_4 and $ZnTiO_3$, the photocatalytical treatments were carried out at an initial pH of around 7.0.

3.3. Photocatalytic activity and kinetics

Evaluating catalytic activity at equal catalyst concentration can lead to inconclusive results since each material may display different optical properties. To address the above limitations, avoiding the precise measurement of the optical properties of the catalysts, the photoactivity of each material can be evaluated at constant volumetric rate of photon absorption in the photoreactor [33]. However, in this work, a comparison of photocatalytic degradation of pirimicarb with ZnO, TiO_2, $ZnTiO_3$ and Zn_2TiO_4 cannot be evaluated at equal level of photon absorption due to large surface particle diameter of Zn_2TiO_4 (4 μm). Therefore, the efficiency of the catalysts in the photooxidation of pirimicarb in optimal conditions was evaluated in view of the work practical nature.

The photocatalytic degradation of pirimicarb using the ZnO–TiO_2 systems was conducted under optimal conditions ([photocatalyst] = 200 mg L^{-1}, pH_0 7.1). The degradation profile of pirimicarb is shown in Fig. 5. The combined action of radiation and the catalyst (UV/TiO_2–ZnO system) leads to the elimination of the insecticide. In the presence of ZnO and TiO_2 P25 Degussa complete disappearance was achieved after 60 min and 30 min of illumination, respectively. The residual levels of pirimicarb after 60 min in the presence of $ZnTiO_3$ and Zn_2TiO_4 were 28 and 57 μg L^{-1}, respectively. In the absence of a catalyst, the photolytic decomposition of pirimicarb occurred at a lower rate than that observed in the photocatalyisis process, and only a 23% reduction of its initial concentration was achieved after 60 min of light exposure.

The kinetic parameters of pirimicarb in optimal conditions are shown in Table 3 where the apparent rate constants and half-lives are listed. The degradation fitted well the exponential decay curve, following first-order behaviour consistent to the Langmuir–Hinshelwood model with R^2 ranging from 0.958 to 1.000. The half-lives for this compound in the presence of TiO_2, ZnO, $ZnTiO_3$ and Zn_2TiO_4 were about 0.6, 3.8, 37.7 and 68.0 min, respectively.

Comparison of TiO_2–ZnO systems showed that TiO_2 is the most efficient for catalyzing the removal of this insecticide. $ZnTiO_3$ and Zn_2TiO_4 appear to be less effective than ZnO and TiO_2, although it can be used as photocatalyst for the pirimicarb oxidation. The absorption threshold of photocatalysts might be responsible for the observed higher rates in ZnO and TiO_2. The corresponding absorption threshold of ZnO, TiO_2, and Zn_2TiO_4 are 413, 400 and 376 nm, respectively, suggesting that ZnO and TiO_2 absorbs a large fraction of UV, and probably absorbed more photons than Zn_2TiO_4 from the light source used (Fig. 3). In addition, Zn_2TiO_4 exhibits a much minor specific surface area than the other photocatalysts (Table 2). $ZnTiO_3$ has smaller band gap (2.8 eV) which permits rapid recombination of hole and electron and so conduction band electron in this semiconductor cannot move into the electron acceptors in the solution rapidly. The photocatalytic activity of semiconductors is also dependent on the crystallinity, particle size,

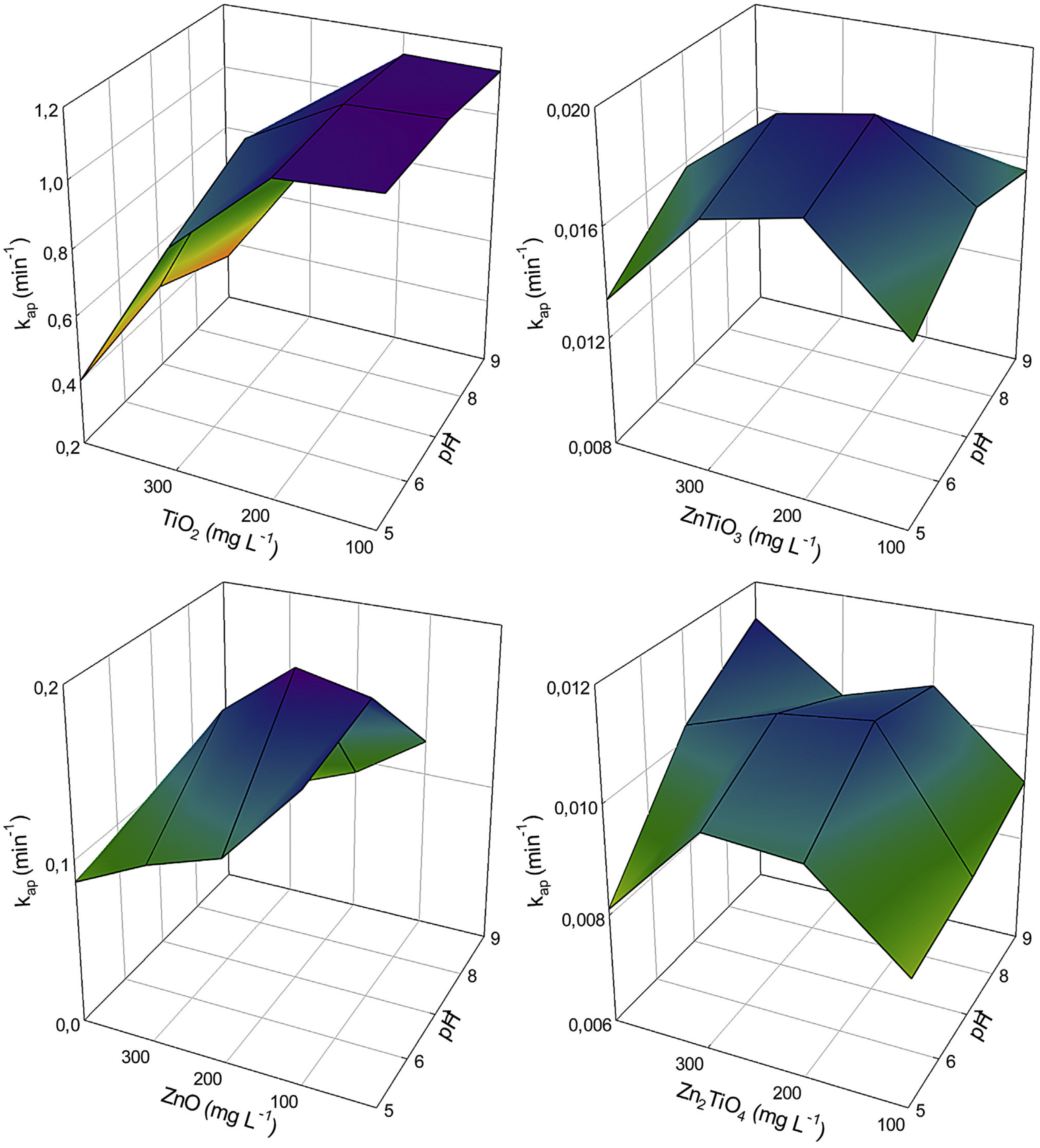

Fig. 4. Optimization of semiconductor (TiO_2 P25 Degussa, ZnO, $ZnTiO_3$ and Zn_2TiO_4) load and initial pH for photocatalytic degradation of pirimicarb (0.1 mg L^{-1}) using a response surface diagram.

surface area and concentration of the impurities in the catalysts [34]. The found photocatalytic activity order ($TiO_2 > ZnO$) agreed with the previously reported [35–38]. Besides that aqueous solutions of pirimicarb are unstable to UV light, the main reason for the greater activity of TiO_2 can be due to its smaller size. Therefore it exhibits a much larger specific surface area than ZnO for applications using artificial light (Table 2). However numerous works have reported that ZnO presents a better efficiency for catalyzing the removal of organic pollutants than that exhibited by TiO_2 for solar applications [20,39,40]. It is due to large fraction absorption of the solar spectrum [26]. In addition, electronic mobility in ZnO is much higher, indicating lower charge recombination [41]. In addition, ZnO has the disadvantage of undergoing photodissolution (induced by self-oxidation). However, this problem can be solved by adjusting the pH of solution to about 9.5 [32].

Although decay in the DOC was observed during the irradiation time, 11% and 8% of the organic carbon was still present after 60 min in ZnO and TiO_2, respectively. These percentages should be due to the formation of non-degradable organic transformation products produced during the experiments and/or other organic compounds present in the commercial insecticide sample.

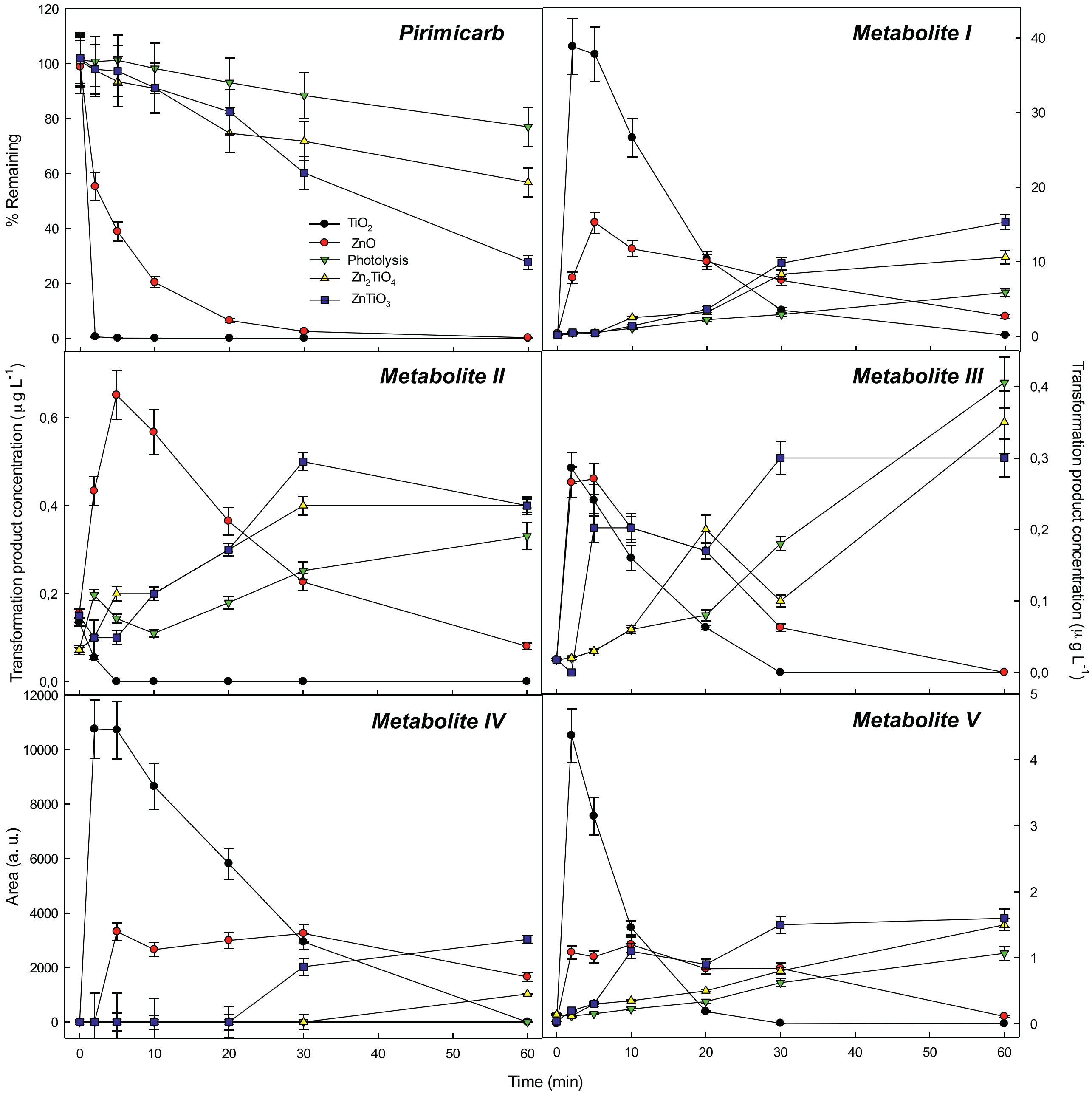

Fig. 5. Degradation kinetics of the pirimicarb and quantitative analysis of derivatives detected in water by photolysis and heterogeneous photocatalysis (TiO_2 P25 Degussa, ZnO, $ZnTiO_3$ and Zn_2TiO_4) during the photoperiod.

3.4. Identification and evolution of the organic transformation products

The transformation of pirimicarb under photolysis or photocatalysis processes leads to the formation of several products. The identification of the most relevant is a very important task to predict the environmental impact of the original compound or to evaluate the efficiency of the photocatalytic treatment. In order to investigate and elucidate the yielded transformation products during pirimicarb degradation, concentrated SPE extracts of the samples, collected at different illumination times, were analyzed by HPLC-MS^2 and HPLC-TOF/MS. Four transformation products (Metabolites I, II, III, V) were isolated and identified by comparison with authentic analytical standards using quantitative HPLC-MS^2. These transformation products were also identified in published papers [42–44].

In addition, after detailed examination of all the peaks present in the chromatograms obtained by HPLC-TOF/MS, five compounds (Metabolites I, II, III, IV, V) were identified as possible transformation products based on their accurate mass and the information provided by the system software, which calculates the elemental

Table 3
Kinetic parameters for photocatalysis (TiO_2, ZnO, Zn_2TiO_4 and $ZnTiO_3$) of pirimicarb in water under artificial light.

Semiconductor	$C_t = C_0 e^{k' t}$	R^2	$S_{y/x}$[a]	$t_{1/2}$ (min)
TiO_2	$C_t = 100.7\ e^{-1.155\ t}$	1.000	0.11	0.6
ZnO	$C_t = 93.6\ e^{-0.183\ t}$	0.978	5.86	3.8
Zn_2TiO_4	$C_t = 98.9\ e^{-0.010\ t}$	0.966	3.31	67.9
$ZnTiO_3$	$C_t = 105.7\ e^{-0.018\ t}$	0.958	6.03	37.7

[a] Standard deviation of the fitting (standard error of estimate).

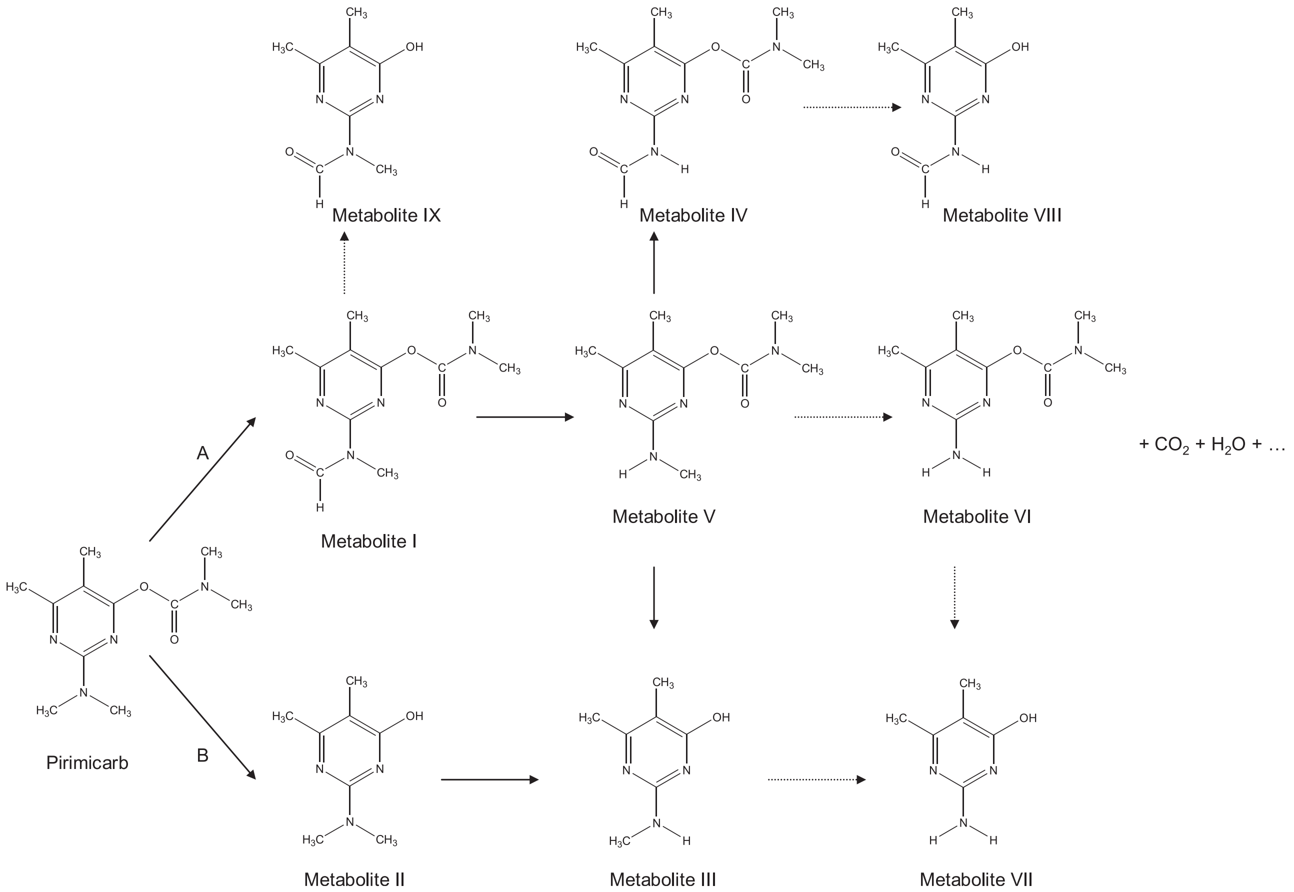

Fig. 6. Photocatalytic degradation pathways of pirimicarb. See Table 1 for identification of derivative compounds (dotted arrows connect transformation products not identified).

composition and empirical formula of protonated molecules, with an accuracy threshold of 5 ppm (standard for unknown identification) and the number of rings and double bonds present in the molecule (DBE, double-bond equivalency). Therefore, a new compound (Metabolite IV) was identified as possible transformation product in addition to those identified by HPLC-MS^2. Table 1 shows summary data related to the experimental and calculated masses of the protonated ion, the error between them and the DBE. Experimental and calculated masses of the protonated ion corresponding to the transformation product identified (Metabolite IV) were 239.1136 and 239.1139, respectively. Accurate mass of transformation product was found with an error of less than 0.93 ppm, thus providing a high degree of certainty in the assignment of formula ($C_{10}H_{14}N_4O_3$). In addition, MS/MS experiment was conducted through the selection of the ions *m*/*z* 72 and 166. We suggest the tentative assignment of this formula with the compound 2-(formylamino)-5,6-dimethylpyrimidin-4-yl dimethylcarbamate. This compound was also identified by Pirisi et al. [42] in aqueous solutions or solid phase of pirimicarb exposed to sunlight or lamps in the laboratory. Other transformation products as 2-amino-5,6-dimethylpyrimidine-4-yl dimethylcarbamate (Metabolite VI), 2-amino-5,6-dimethyl-4-hydroxypyrimidine (Metabolite VII), 2-(formylamino)-5,6-dimethyl-4-hydroxypyrimidine (Metabolite VIII) and 2-[(methylformyl) amino]-5,6-dimethyl-4-hydroxypyrimidine (Metabolite IX) were not detected by HPLC-TOF/MS.

Little information is available comparing the photodegradation route of pirimicarb in aqueous suspension of ZnO–TiO_2 systems. In order to better understand the reaction mechanisms involved in the photocatalytic degradation of pirimicarb, the kinetic evolution of principal transformation products was also followed during the irradiation experiment (Fig. 5). The rapid transformation of pirimicarb was accompanied by the appearance of five transformation products. On the one hand, TiO_2 and ZnO treatments led to similar evolution profiles for most of the obtained transformation products but different from those observed for $ZnTiO_3$ and Zn_2TiO_4 catalysts whose effect on the metabolite profile were similar to that showed with the photolysis treatment. The most abundant transformation product was Metabolite I followed by Metabolite V and Metabolite IV. Metabolite I was detected in concentrations of 15 $\mu g\,L^{-1}$ for ZnO (after 5 min), 39 $\mu g\,L^{-1}$ for TiO_2 (after 2 min), 15 $\mu g\,L^{-1}$ for $ZnTiO_3$ (after 60 min) and 11 $\mu g\,L^{-1}$ for Zn_2TiO_4 (after 60 min). In the case of TiO_2, only Metabolite I was found in the medium at the end of the experiment (60 min). Observed differences in the concentration of the transformation products found for ZnO–TiO_2 systems may be due to the different reaction rates obtained. Based on the results, a possible photocatalytic degradation pathway of pirimicarb consisting of several steps was proposed in Fig. 6. As can be seen, all the transformation products are formed in mainly two different ways: In the first case, through successive N-dealkylation of the 2-dimethylamino group to form the carbamate (step A). In the second case, through decarbamoylation of the carbamate moiety with further N-dealkylation of the 2-dimethylamino group to have the hydroxypyrimidines (step B).

4. Conclusions

The photodegradation of pirimicarb in aqueous suspensions of binary (ZnO and TiO_2) and ternary (Zn_2TiO_4 and $ZnTiO_3$) oxides of zinc and titanium under artificial light (300–460 nm) irradiation was investigated. Pirimicarb was totally degraded in aqueous suspensions of ZnO and TiO_2 under artificial light irradiation (300–460 nm) after 60 and 30 min, respectively. In general, the efficiency of the catalysts in the photooxidation of pirimicarb was in the order: $TiO_2 > ZnO > ZnTiO_3 > Zn_2TiO_4$. However, the process using ZnO would present drawbacks in comparison with TiO_2 since the pH must be adjusted to precipitate the Zn^{2+} and then be neutralized to be released in the environment, as it is the case with Fe in photo-Fenton process. Five transformation products were identified by HPLC-MS^2 and HPLC-TOF/MS during the experiments. Based on this derivative identification, a simple degradation pathway, mainly trough dealkylation and decarbamoylation, is proposed for the parent compounds.

Acknowledgements

We acknowledge financial support from the Ministerio de España de Ciencia e Innovación (Project AGL2010-20458-C02-01), Ramón and Cajal Subprogram and the Instituto Nacional de Investigación y Tecnología Agraria y Alimentaria (Project RTA2011-00022-00-00). We are also grateful to Inmaculada Garrido, Juana Cava, María V. Molina and María J. Yáñez for technical assistance and to FEDER and European Social Funds.

References

[1] C.D.S. In: Tomlin (Ed.), The Pesticide Manual, 15th ed., British Crop Protection Council: Surrey, 2009.

[2] J. Zhou, C. Ma, S. Zhou, P. Ma, F. Chen, Y. Qi, H. Chen, Preparation, evaluation and application of molecularly imprinted solid-phase microextraction monolith for selective extraction of pirimicarb in tomato and pear, J. Chromatogr. A 1217 (2010) 7478–7483.

[3] J. Fenoll, E. Ruiz, P. Flores, P. Hellin, S. Navarro, Leaching potential of several insecticides and fungicides through disturbed clay–loam soil columns, Int. J. Environ. Anal. Chem. 90 (2010) 276–285.

[4] E.R. Taboada, A. Dekker, A. van Kammen-Polman, J.H. Smelt, J.J.T.I. Boesten, M. Leistra, Adsorption, degradation and leaching of pirimicarb in orchard soils, Sci. Total Environ. 153 (1994) 253–260.

[5] S. Navarro, J. Fenoll, N. Vela, E. Ruiz, G. Navarro, Photocatalytic degradation of eight pesticides in leaching water by use of ZnO under natural sunlight, J. Hazard. Mater. 172 (2009) 1303–1310.

[6] S. Malato, P. Fernández-Ibañez, M.I. Maldonado, J. Blanco, W. Gernjak, Decontamination and disinfection of water by solar photocatalysis: recent overview and trends, Catal. Today 147 (2009) 1–59.

[7] S. Ahmed, M.G. Rasul, R. Brown, M.A. Hashib, Influence of parameters on the heterogeneous photocatalytic degradation of pesticides and phenolic contaminants in wastewater: a short review, J. Environ. Manag. 92 (2011) 311–330.

[8] Y.F. Rao, W. Chu, Linuron decomposition in aqueous semiconductor suspension under visible light irradiation with and without H_2O_2, Chem. Eng. J. 158 (2010) 181–187.

[9] J. Fenoll, P. Flores, P. Hellín, C.M. Martínez, S. Navarro, Photodegradation of eight miscellaneous pesticides in drinking water after treatment with semiconductor materials under sunlight at pilot plant scale, Chem. Eng. J. 204–206 (2012) 54–64.

[10] S. Ahmed, M.G. Rasul, W.N. Martens, R. Brown, M.A. Hashib, Advances in heterogeneous photocatalytic degradation of phenols and dyes in wastewater: a review, Water Air Soil Pollut. 215 (2011) 3–29.

[11] M.N. Chong, B. Jin, C.W.K. Chow, C. Saint, Recent developments in photocatalytic water treatment technology: a review, Water Res. 44 (2010) 2997–3027.

[12] J.M. Herrmann, Heterogeneous photocatalysis: state of the art and present applications in honor of Pr. R.L. Burwell Jr. (1912–2003) former head of Ipatieff Laboratories Northwestern University, Evanston (Ill), Top Catal. 34 (2005) 49–65.

[13] I.K. Konstantinou, T.A. Albanis, Photocatalytic transformation of pesticides in aqueous titanium dioxide suspensions using artificial and solar light: intermediates and degradation pathways, Appl. Catal. B 42 (2003) 319–335.

[14] M.G. Antoniou, J.A. Shoemaker, A.A. De La Cruz, D.D. Dionysiou, Unveiling new degradation intermediates/pathways from the photocatalytic degradation of microcystin-LR, Environ. Sci. Technol. 42 (2008) 8877–8883.

[15] D. Chatterjee, S. Dasgupta, N.N. Rao, Visible light assisted photodegradation of halocarbons on the dye modified TiO_2 surface using visible light, Sol. Energy Mater. Sol. Cells 90 (2006) 1013–1020.

[16] M.C. Yeber, J. Rodriguez, J. Freer, N. Durán, H.D. Mansilla, Photocatalytic degradation of cellulose bleaching effluent by supported TiO_2 and ZnO, Chemosphere 41 (2000) 1193–1197.

[17] T. Deguchi, K. Imai, H. Matsui, M. Iwasaki, H. Tada, S.J. Ito, Rapid electroplating of photocatalytically highly active TiO_2–Zn nanocomposite films on steel, Mater. Sci. 36 (2001) 4723–4729.

[18] Y. Wang, P. Yuan, C. Fan, Y. Wang, G. Ding, Y.F. Wang, Preparation of zinc titanate nanoparticles and their photocatalytic behaviors in the photodegradation of humic acid in water, Ceram. Int. 38 (2012) 4173–4180.

[19] F. Seitz, M. Bundschuh, A. Dabrunz, N. Bandow, G.E. Schaumann, R. Schulz, Titanium dioxide nanoparticles detoxify pirimicarb under UV irradiation at ambient intensities, Environ. Toxicol. Chem. 31 (2012) 518–523.

[20] J. Fenoll, P. Sabater, G. Navarro, G. Pérez-Lucas, S. Navarro, Photocatalytic transformation of sixteen substituted phenylurea herbicides in aqueous semiconductor suspensions: intermediates and degradation pathways, J. Hazard. Mater. 244–245 (2013) 370–379.

[21] J. Fenoll, P. Hellin, C.M. Martinez, P. Flores, S. Navarro, Determination of 48 pesticides and their main metabolites in water samples by employing sonication and liquid chromatography-tandem mass spectrometry, Talanta 85 (2011) 975–982.

[22] Z. Ali, S. Ali, I. Ahmad, I. Khan, H.A. Rahnamaye Aliabad, Structural and optoelectronic properties of the zinc titanate perovskite and spinel by modified Becke–Johnson potential, Phys. Rev. B Condens. Matter 420 (2013) 54–57.

[23] P.K. Jain, D. Kumar, A. Kumar, D. Kaur, Structural, optical and dielectric properties of $ZnTiO_3$ ceramics, Optoelectron. Adv. Mat. 4 (2010) 299–304.

[24] G.S. Pozan, A. Kambur, Significant enhancement of photocatalytic activity over bifunctional ZnO–TiO_2 catalysts for 4-chlorophenol degradation, Chemosphere 105 (2014) 152–159.

[25] M.A. Valenzuela, P. Bosch, J. Jiménez-Becerrill, O. Quiroz, A.I. Páez, Preparation, characterization and photocatalytic activity of ZnO Fe_2O_3 and $ZnFe_2O_4$, J. Photochem. Photobiol. A 148 (2002) 177–182.

[26] S. Sakthivel, B. Neppolian, M.V. Shankar, B. Arabindoo, M. Palanichamy, V. Murugesan, Solar photocatalytic degradation of azo dye: comparison of photocatalytic efficiency of ZnO and TiO_2, Sol. Energy Mater. Sol. Cells 77 (2003) 65–82.

[27] A. Fujishima, T.N. Rao, A.D. Tryk, Titanium dioxide photocatalysis, J. Photochem. Photobiol. C 1 (2000) 1–21.

[28] S. Rabindranathan, S. Devipriya, S. Yesodharan, Photocatalytic degradation of phosphamidon on semiconductor oxides, J. Hazard. Mater. B 102 (2003) 217–229.

[29] M. Kosmulki, The pH-dependent surface charging and points of zero charge: V. Update, J. Colloid Interface Sci. 353 (2011) 1–15.

[30] E. Vulliet, J.M. Chovelon, C. Guillard, J.M. Herrmann, Factors influencing the photocatalytic degradation of sulfonylurea herbicides by TiO_2 aqueous suspension, J. Photochem. Photobiol. A 159 (2003) 71–79.

[31] J. Fenoll, P. Sabater, G. Navarro, N. Vela, G. Pérez-Lucas, S. Navarro, Abatement kinetics of 30 sulfonylurea herbicide residues in water by photocatalytic treatment with semiconductor materials, J. Environ. Manag. 130 (2013) 361–368.

[32] J. Fenoll, P. Hellin, C.M. Martinez, P. Flores, S. Navarro, Semiconductor oxides-sensitized photodegradation of fenamiphos in leaching water under natural sunlight, Appl. Catal. B 115–116 (2012) 31–37.

[33] D. Dolat, N. Quici, E. Kusiak-Nejman, A.W. Morawski, G.L. Puma, One-step hydrothermal synthesis of nitrogen carbon co-doped titanium dioxide (N, C_TiO_2) photocatalysts. Effect of alcohol degree and chain length as carbon dopant precursors on photocatalytic activity and catalyst deactivation, Appl. Catal. B 115 (2012) 81–89.

[34] N.H. Salah, M. Bouhelassa, S. Bekkouche, A. Boultif, Study of photocatalytic degradation of phenol, Desalination 166 (2004) 347–354.

[35] B. Swarnalatha, Y. Anjaneyulu, Studies on the heterogeneous photocatalytic oxidation of 2,6-dinitrophenol in aqueous TiO_2 suspension, J. Mol. Catal. A Chem. 223 (2004) 161–165.

[36] L. Poulios, M. Kositzi, K. Pitarakis, S. Beltsios, I. Oikonomou, Photocatalytic oxidation of methomyl in the presence of semi conducting oxides, Int. J. Environ. Pollut. 28 (2006) 33–44.

[37] M. Qamar, M. Muneer, A comparative photocatalytic activity of titanium dioxide and zinc oxide by investigating the degradation of vanillin, Desalination 249 (2009) 535–540.

[38] M.A. Valenzuela, P. Bosch, J. Jiménez-Becerrill, O. Quiroz, A.I. Páez, Preparation, characterization and photocatalytic activity of ZnO Fe_2O_3 and $ZnFe_2O_4$, J. Photochem. Photobiol. A 148 (2002) 177–182.

[39] J. Fenoll, P. Hellin, P. Flores, C.M. Martinez, S. Navarro, Degradation intermediates and reaction pathway of carbofuran in leaching water using TiO_2 and ZnO as photocatalyst under natural sunlight, J. Photochem. Photobiol. A 251 (2013) 33–40.

[40] N. Daneshvar, D. Salari, A.R. Khataee, Photocatalytic degradation of azo dye acid red 14 in water on ZnO as an alternative catalyst to TiO_2, J. Photochem. Photobiol. A 162 (2004) 317–322.

[41] V. Kitsiou, N. Filippidis, D. Mantzavinos, I. Pouios, Heterogeneous and homogeneous photocatalytic degradation of the insecticide imidacloprid in aqueous solutions, Appl. Catal. B 86 (2009) 27–35.

[42] F.M. Pirisi, P. Cabras, V.L. Garau, M. Melis, E. Secchi, Photodegradation of pesticides. Photolysis rates and half-life of pirimicarb and its metabolites in reactions in water and in solid phase, J. Agric. Food Chem. 44 (1996) 2417–2422.

[43] P. Cabras, M. Melis, F. Cabitza, M. Cubeddu, L. Spanedda, Persistence of pirimicarb in peaches and nectarines, J. Agric. Food Chem. 43 (1995) 2279–2282.

[44] E. Romero, P. Schmitt, M. Mansour, Photolysis of pirimicarb in water under natural and simulated sunlight conditions, Pestic. Sci. 41 (1994) 21–26.